

# Multi-Atom Resonant Photoemission Effects from Solid Surfaces and Free Molecules

N. Mannella<sup>1,2</sup>, B.S. Mun<sup>1,2</sup>, S.-H. Yang<sup>2</sup>, A.W. Kay<sup>1,2,#</sup>, F.J. Garcia de Abajo<sup>1,3</sup>,  
E. Arenholz<sup>4</sup>, A.T. Young<sup>4</sup>, Z. Hussain<sup>4</sup>, H. Wang<sup>5</sup>, O. Hemmers<sup>5</sup>,  
D.W. Lindle<sup>5</sup>, M.A. Van Hove<sup>1,2</sup>, and C.S. Fadley<sup>1,2</sup>

<sup>1</sup>Dept. of Physics, University of California-Davis, Davis, CA 95616

<sup>2</sup>Materials Sciences Division, Lawrence Berkeley National Laboratory, Berkeley, CA 94720

<sup>3</sup>Centro Mixto CSIC-UPV/EHU, San Sebastian, Spain

<sup>4</sup>Advanced Light Source, Lawrence Berkeley National Laboratory, Berkeley, CA 94720

<sup>5</sup>Dept. of Chemistry, University of Nevada, Las Vegas, NV 89154

<sup>#</sup>Present address: Intel Corporation, Portland, OR

## INTRODUCTION

In prior work at the ALS, it has been pointed out that a new type of interatomic resonant photoemission effect exists, and that this effect furthermore has the potential of providing a useful probe of near-neighbor atomic identities, bonding, and magnetism [1-5]. The phenomenon has been termed multi-atom resonant photoemission (MARPE). In measuring this effect, the photoelectron intensity of a given core level from atom "A" (e.g. O 1s from MnO) is monitored while the photon energy is tuned through a strong absorption edge for a core level on another atom "B" in the sample (e.g. the Mn 2p edges in MnO). Initial observations on MnO and other metal oxides appeared to show significant entirely-positive interatomic resonant effects in photoemission of up to 100% [1]. Additional measurements in Auger emission and soft x-ray emission from MnO seemed to confirm that such effects were also present in secondary decay processes as a result of resonant enhancement of the initial O 1s core hole formation [2]. A theoretical model for these effects based on the extension of intraatomic resonant photoemission ideas to the interatomic case was also developed and compared favorably with experiment [3]. Other measurements on transition-metal compounds [6] and an adsorbate-substrate system [7a] seemed to confirm these measurements and analysis.

Subsequently, it has been realized that such experimental measurements require very careful allowance for potential detector non-linearities [4,5,7b], since the observed electron intensities (particularly inelastically scattered backgrounds) change dramatically in going over any core resonance. In particular, the detector used for several of the first MARPE studies [1,2,4-7a], the standard microchannel plate-plus-phosphor-plus-CCD camera incorporated in the Gammadata-Scienta series of electron spectrometers, exhibits not only a typical saturation effect for high countrates, but also a strong quadratic component of counting that goes above linear for low countrates. Thus, spectra obtained in this low-countrate regime, while not exhibiting any kind of saturation effect, can be artificially enhanced in intensity in passing over a core-level resonance. Methods of accurately correcting spectra for these non-linearities have been discussed [4,5,7b, and abstract by Mannella et al. in this 2001 Compendium]. When these effects are allowed for, the magnitude of the effect is reduced and the form is found to change, with the shape usually involving a negative-then-positive swing in intensity reminiscent of a Fano profile in form [4,5,7b,8].

We here report more recent experimental results providing further evidence of such interatomic resonant effects in photoemission, for two very different limiting-case types of systems: a cleaved single-crystal oxide-NiO and a free molecule-SF<sub>6</sub>. These data are discussed in terms of existing theoretical models for such MARPE effects [3,5], in particular, an x-ray optical (dielectric) approach that well describes the NiO data and a microscopic quantum mechanical model that should be useful in describing the SF<sub>6</sub> data.

## EXPERIMENTAL PROCEDURE

The NiO measurements were performed on beamline 4.0.2 and made use of the Advanced Photoelectron Spectrometer/Diffractometer located there. Detector non-linearities were corrected for in all data presented here, using methods described elsewhere [4,5, and abstract in the 2001 Compendium]. A NiO single crystal was cleaved just before insertion into ultrahigh vacuum via a loadlock, then ion bombardment and annealing in oxygen to remove minor surface contaminant levels and assure correct stoichiometry before measurement. The incidence angle of the radiation was varied from grazing values of 5° to much higher values up to 40° (cf. experimental geometry in Figure 1(a)).

The SF<sub>6</sub> measurements were performed on beamline 8.0.1 and made use of a time-of-flight spectrometer described in detail elsewhere [9]. The detectors in this spectrometer are positioned in angle with respect to the incoming radiation and polarization vector such that non-dipole contributions to the angular distributions can be readily measured with high accuracy. For reference, the angular distributions of photoelectrons from a randomly oriented ensemble of free molecules is given by  $d\sigma/d\Omega = (\sigma/4\pi)\{1 + \beta P_2(\cos\Theta_e) + [\delta + \gamma \cos^2\Theta_e] \sin\Theta_e \cos\Phi_e\}$ , with  $\beta$  the dipole asymmetry parameter and  $\delta$  and  $\gamma$  the first-order non-dipole parameters (cf. geometry in Figure 2(a), with  $\Phi_e$  being the azimuthal angle around the polarization vector  $\epsilon$ ) [9].

## EXPERIMENTAL RESULTS AND DISCUSSION

**NiO(001):** In Figure 1, we show experimental O 1s intensities from NiO as a function of photon energy and for five different x-ray incidence angles. For the lowest incidence angle of 5°, the effect of crossing the Ni 2p absorption resonances is dramatic, yielding a negative-then-positive excursion on crossing 2p<sub>3/2</sub> whose amplitude is 75% of the intensity below the resonance. The magnitudes of these effects decreases as the incidence angle is increased, falling off to about 5% for an incidence angle of 40°.

Also shown in Figure 1 are theoretical curves based on an x-ray optical model of such effects, as discussed previously [5]. The optical constants that are key inputs for this model have been derived from concomitant partial-yield x-ray absorption measurements, with corrections for x-ray incidence angle and secondary electron takeoff angle [4], and subsequent Kramers-Kronig analysis [5]. The resulting theoretical curves are in excellent agreement with experiment for the lowest angle, and the agreement is very good for all other angles as well, although with some overprediction of the amplitudes at the higher angles. Non-zero effects are observed and predicted over the full angle range, in qualitative agreement with prior data for MnO [5]. These data thus disagree with one aspect of an earlier study of NiO by Finazzi et al. [8], in which they did not observe any sort of MARPE effect in O 1s emission from NiO; this lack of any effect appears to be due to measuring with too high an incidence angle and having insufficient statistical accuracy to resolve the small remaining effects seen, e.g. in Figures 2(e)-2(f).

We thus expect such MARPE effects to be observable in photoemission from any solid surface, with strength depending on the relative intensities of the absorption resonances. Furthermore, for homogeneous systems with flat surfaces, the x-ray optical model should provide a reasonably quantitative picture of the observed phenomena. Effects following an x-ray optical analysis have also recently been observed for photoemission from an adsorbate on a metal-N<sub>2</sub>/Ni(001) [10]. For more complex cases with, e.g., three-dimensional nanometer-scale heterogeneity, the use of a microscopic model will be more appropriate.

**SF<sub>6</sub>:** In Figure 2, experimental results for SF<sub>6</sub> are summarized. The x-ray absorption coefficient is shown in Figure 2(b), and the S 2p photoemission intensity and its asymmetry parameters were measured as photon energy was scanned across the "A" absorption resonance (corresponding to a F

1s  $t_{1u}$ -to- $a^*_{1g}$  excitation). Although the total S 2p intensity (proportional to  $\sigma$ ) does not show a significant change in crossing the resonance ( $\leq$ few %), the dipole asymmetry parameter  $\beta$  (as shown in Figure 2(b)) exhibits about a 15% excursion in magnitude that is also of the same general form as those in Figure 1. Similar effects are also seen in the parameters  $\delta$  and  $\gamma$ [11].

Thus, interatomic resonant effects are also seen in this free molecule, and although they are too small to be observed as yet in the total intensity, they are clearly observed in the various asymmetry parameters. No theoretical calculations have as yet been performed for this case, but the x-ray optical model would clearly be inappropriate, and a microscopic approach such as that discussed previously [3,5] is the logical starting point for understanding these effects.

## CONCLUSIONS

Multi-atom resonant photoemission effects are found in both the total intensities from homogeneous solid surfaces and adsorbates on such surfaces, for which an x-ray optical model is found to well describe the data, and in the angular distribution asymmetry parameters of a free molecule, for which a microscopic theoretical approach will be necessary. Similar effects in nanoscale structures will lie somewhere between these two cases.

## REFERENCES

1. A. Kay, E. Arenholz, B.S. Mun, F.J. Garcia de Abajo, C.S. Fadley, R. Denecke, Z. Hussain, and M.A. Van Hove, *Science* **281**, 679(1998).
2. (a) E. Arenholz, A.W. Kay, C.S. Fadley, M.M. Grush, T.A. Callcott, D.L. Ederer, C. Heske, and Z. Hussain, *Phys. Rev. B* **61**, 7183 (2000); (b) E. Arenholz, A.W. Kay, unpublished results.
3. F.J. Garcia de Abajo, C.S. Fadley, and M.A. Van Hove, *Phys. Rev. Lett.* **82**, 4126 (1999).
4. A.W. Kay, Ph.D. dissertation (University of California-Davis, September, 2000), Chapters 4 and 5.
5. A.W. Kay, F.J. Garcia de Abajo, S.H. Yang, E. Arenholz, B.S. Mun, M.A. Van Hove, Z. Hussain, and C.S. Fadley, *Physical Review B* **63**, 5119 (2001).
6. A. Kikas, E. Nommiste, R. Ruus, A. Saar, and I. Martinson, *Sol. St. Commun.* **115**, 275 (2000).
7. (a) M.G. Garnier, N. Witkowski, R. Denecke, D. Nordlund, A. Nilsson, M. Nagasono, and N. Mårtensson, and A. Föhlisch, Maxlab Annual Report for 1999 and private communication correcting this data; (b) D. Nordlund, M. G. Garnier, N. Witowsky, R. Denecke, A. Nilsson, M. Nagasono, N. Mårtensson and A. Föhlisch, *Phys. Rev. B* **63**, 121402 (2001).
8. M. Finazzi, G. Ghiringhelli, O. Tjernberg, L. Duo, A. Tagliaferri, P. Ohresser, and N. B. Brookes, *Phys. Rev. B* **62**, R16215 (2000).
9. (a) O. Hemmers et al., *Rev. Sci. Instrum.* **69**, 3809 (1998); (b) O. Hemmers et al., *Phys. Rev. Lett.* **87**, 273003 (2001).
10. D. Menzel, W. Wurth, A. Föhlisch, P. Fuelner, S.-H. Yang, and C.S. Fadley, private communication.
11. H. Wang, O. Hemmers, P. Focke, M. M. Sant'Anna, D. Lukic, C. Heske, R. C. C. Perera, I. Sellin, and D. Lindle, to be published.

This work was supported by the U.S. Department of Energy, Office of Science, Office of Basic Energy Sciences, Materials Sciences Division, under Contract No. DE-AC03-76SF00098, and the National Science Foundation.

Principal investigator: N. Mannella, Department of Physics UC Davis, and Materials Sciences Division, Lawrence Berkeley National Laboratory. Email: norman@electron.lbl.gov. Telephone: 510-486-4581

Figure 1. (a) Experimental geometry for measurements on Ni(001). (b)-(f) O 1s intensity as photon energy is scanned through the Ni 2p<sub>1/2-3/2</sub> absorption resonances. Both experimental data (blue points) and theoretical calculations based on an x-ray optical model (red curves) are shown.

Figure 2. (a) Experimental geometry for measurements on gas-phase SF<sub>6</sub>. (b) The x-ray absorption coefficient in the F 1s region as measured by partial electron yield. (c) The dipole asymmetry parameter  $\beta$  as photon energy is scanned through the "A" resonance in (b).

Figure 1.

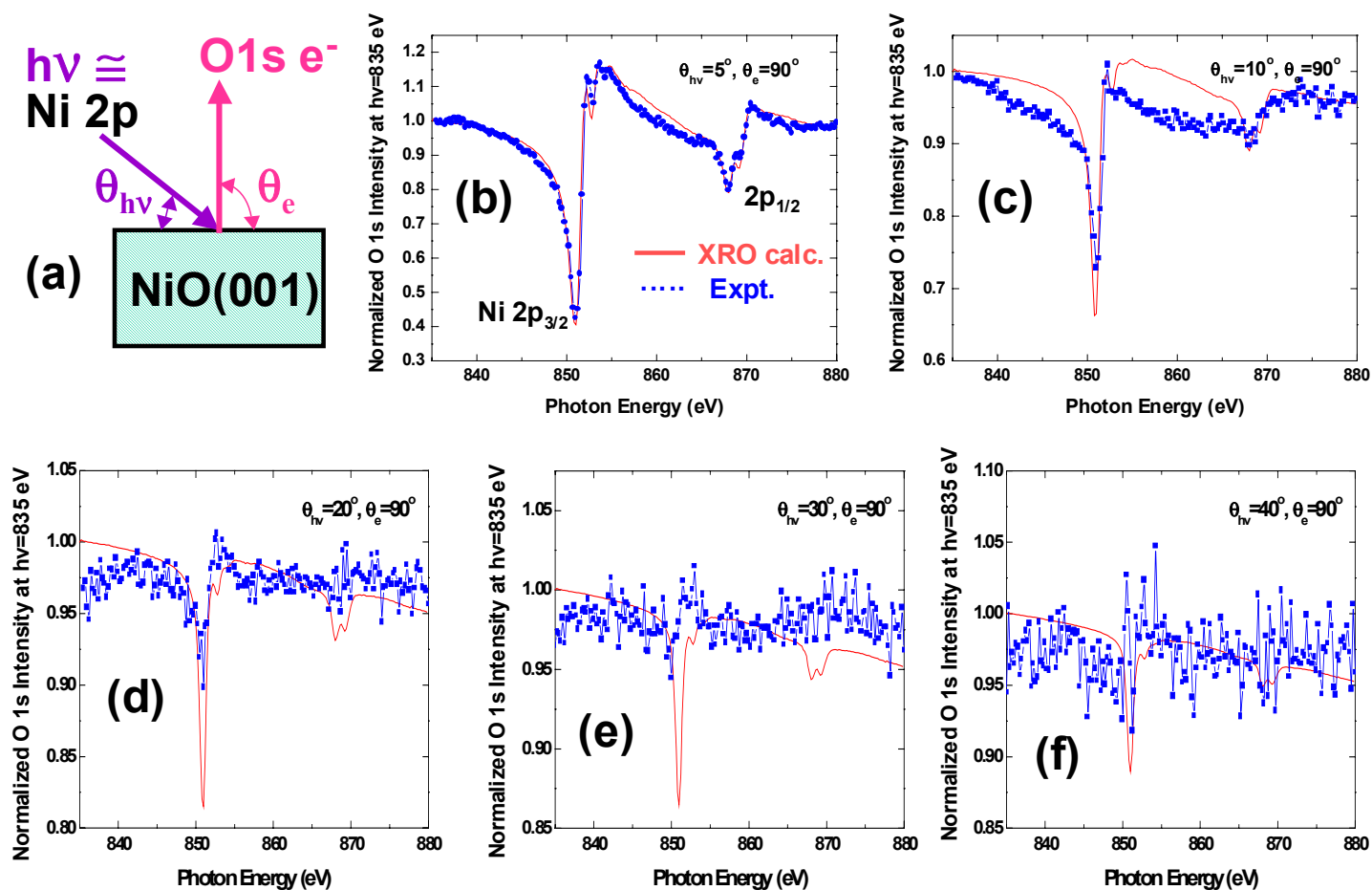


Figure 2.

